

Highlights

Dynamic Spatio-Temporal Summarization using Information Based Fusion

Humayra Tasnim, Soumya Dutta, Melanie Moses

- The research introduces a novel and adaptable method for interpreting informative features of large scale spatiotemporal data, applicable to diverse datasets from different domains.
- The proposed technique identifies key informative timesteps and uses information-based fusion to summarize salient patterns of important features in less informative timesteps, leading to significant storage optimization without compromising data insights.
- Proposed approach facilitates effective visualization, tracking, and analysis of temporal changes in the datasets.

Dynamic Spatio-Temporal Summarization using Information Based Fusion

Humayra Tasnim^{a,*}, Soumya Dutta^b and Melanie Moses^a

^aUniversity of New Mexico, Albuquerque, New Mexico, 87131, United States

^bIndian Institute of Technology Kanpur, Uttar Pradesh, 208016, India

ARTICLE INFO

Keywords:

Information Theory
Specific Mutual Information
Data Fusion
Spatio-temporal Fusion
Data Summarization
Data Visualization
Time-Varying Data

ABSTRACT

In the era of burgeoning data generation, managing and storing large-scale time-varying datasets poses significant challenges. With the rise of supercomputing capabilities, the volume of data produced has soared, intensifying storage and I/O overheads. To address this issue, we propose a dynamic spatio-temporal data summarization technique that identifies informative features in key timesteps and fuses less informative ones. This approach minimizes storage requirements while preserving data dynamics. Unlike existing methods, our method retains both raw and summarized timesteps, ensuring a comprehensive view of information changes over time. We utilize information-theoretic measures to guide the fusion process, resulting in a visual representation that captures essential data patterns. We demonstrate the versatility of our technique across diverse datasets, encompassing particle-based flow simulations, security and surveillance applications, and biological cell interactions within the immune system. Our research significantly contributes to the realm of data management, introducing enhanced efficiency and deeper insights across diverse multidisciplinary domains. We provide a streamlined approach for handling massive datasets that can be applied to in situ analysis as well as post hoc analysis. This not only addresses the escalating challenges of data storage and I/O overheads but also unlocks the potential for informed decision-making. Our method empowers researchers and experts to explore essential temporal dynamics while minimizing storage requirements, thereby fostering a more effective and intuitive understanding of complex data behaviors.

1. Introduction

In today's data-driven world, the exponential growth in data generation has brought forth significant challenges for storage and associated I/O overheads. Modern supercomputing capabilities have reduced the computational cost of producing data, resulting in the creation of massive datasets at an accelerating pace [Reed and Dongarra (2015); Childs (2015)]. Many of these datasets exhibit a dynamic temporal nature, consisting of multiple timesteps that may be redundant or offer minimal new information when analyzed timestep by timestep. The storage burden of retaining these less informative timesteps poses a critical issue, calling for novel techniques that can efficiently manage such large-scale time-varying datasets.

To address this challenge, we propose a data summarization technique that aims to minimize the storage overhead while preserving the vital temporal dynamics of the dataset. We also emphasize visualizing these dynamics by tracking changes over time. Our approach involves a dynamic spatio-temporal technique, which identifies both key timesteps and redundant timesteps. We store the key timesteps and summarize the redundant multiple timesteps into one, highlighting the salient features. The summarization technique effectively ensures storage reduction with

minimal loss. We propose to use information-theoretic measures namely the Specific Mutual Information or SMI-guided fusion for the summaries.

The core idea of the summarization technique is to identify informative temporal features within the redundant timesteps and fuse them using principles from information theory. By selecting the most relevant features from the redundant timesteps and summarizing them through information-guided fusion, we ensure that the temporal dynamics are retained. This approach not only optimizes storage requirements but also facilitates the visualization and tracking of information change over time, providing valuable insights into the underlying data patterns.

In the paper, we present the details of our data summarization technique, dynamic spatio-temporal framework, and the information-guided fusion process. We demonstrate the technique's versatility by applying it to different datasets, including scalar data from particle-based simulations and image data from surveillance footage and cellular interactions. Our results show significant storage reduction without compromising critical insights, proving the effectiveness of our approach for efficient data management and visualization.

Our research aim in this work is to develop a method that efficiently handles large-scale time-varying datasets across various domains. Our solution seeks to bridge the data reduction landscape by providing approaches to effectively manage large and intricate temporal datasets. Our goal is to achieve this while retaining essential features and enabling robust visualization techniques. By leveraging the power of information theory, we aim to contribute to a more efficient

*Corresponding author

✉ htasnim30@unm.edu (H. Tasnim); soumyad@cse.iitk.ac.in (S. Dutta); melaniem@cs.unm.edu (M. Moses)

🌐 htasnim.github.io (H. Tasnim); soumyadutta-cse.github.io (S. Dutta); moseslab.cs.unm.edu (M. Moses)

ORCID(s): 0000-0002-7796-7717 (H. Tasnim); 0000-0001-5030-9979 (S. Dutta)

and insightful data management strategy, especially in the context of dynamic and multifaceted datasets.

The contributions of the paper are:

- Develop a dynamic spatio-temporal summarization (DSTS) technique for large-scale time-varying datasets. The summary provides three features: key timesteps, fused timesteps, and holistic visual representation of information change.
- Propose and demonstrate that the specific mutual information (SMI) measure "Surprise" provides the most promising outcomes for the fusion technique.
- Demonstrate the versatility and effectiveness of the proposed technique (acm) through application to diverse datasets, including chemical simulations, surveillance footage, and cell interactions in the immune system.
- Explore the impact of the technique in optimizing data storage with minimal data loss.

The paper's structure is as follows: Section 2 reviews related works on data summarization and information theory-based approaches. Section 3 outlines the methodology for the framework. Section 4 demonstrates the results of implementing the technique across multi-domain datasets. Section 5 delves into the implications of our findings and the research's importance in diverse application domains. Lastly, Section 6 concludes the paper by highlighting possible future research avenues.

2. Related Works

Efficiently managing and analyzing large-scale time-varying datasets has attracted considerable attention across multiple disciplines, leading to various strategies to address the challenges posed by data growth. In this work, we focus on identifying and storing informative key timesteps while summarizing less informative ones by fusion. The summaries reduce storage overhead while the key and fused timesteps preserve data dynamics. Various data compression and reduction techniques have been explored in the context of large-scale data analysis, aligning with the goals of the proposed research. There are techniques that represent data reduction where reduced data is stored in place of the raw data. Cinema [Ahrens, Jourdain, O'Leary, Patchett, Rogers and Petersen (2014)] is an in situ data reduction and visualization approach that utilizes image-based representations to capture essential features of time-varying datasets. Techniques like lossless and lossy compression methods are commonly used for data reduction. References [Vidhya, Karthikeyan, Divakar and Ezhumalai (2016); Cappello, Di, Li, Liang, Gok, Tao, Yoon, Wu, Alexeev and Chong (2019); Di and Cappello (2016)] present various compression algorithms and their application in handling large datasets. Other reduction technique includes subsampling [Woodring, Ahrens, Figg, Wendelberger, Habib

and Heitmann (2011); Wei, Dutta and Shen (2018)] and distribution-based summaries [Dutta, Chen, Heinlein, Shen and Chen (2016); Ye, Neuroth, Sauer, Ma, Borghesi, Konduri, Kolla and Chen (2016)]. The abovementioned methods are widely recognized for their data reduction and compression effectiveness. However, these approaches solely store the reduced timesteps. In our work, we need to retain both the raw and reduced timesteps to comprehensively capture information changes over time and preserve essential data dynamics.

Identifying key time steps is essential in analyzing time-varying data and advancing scientific visualization. There are numerous approaches [Zhou and Chiang (2018); Myers, Lawrence, Fugate, Bowen, Ticknor, Woodring, Wendelberger and Ahrens (2016); Tong, Lee and Shen (2012); Hu, Xie, Li, Zeng and Maybank (2011)] that have been proposed for identifying key time steps in large time-varying datasets. These studies focus on only capturing key time steps without the summarization capacity. Some studies focused on data reduction such as: in [Akiba, Fout and Ma (2006)] similar timesteps are grouped and one is selected, in Wang, Yu and Ma (2008) salient timesteps were selected by comparing dissimilarity with previous timestep. These studies did not include any summarization techniques which we incorporated in our proposed work along with selecting key time steps.

The development of fusion techniques [Castanedo et al. (2013)] for large-scale spatio-temporal datasets has been a popular field of interest for researchers across various domains like remote sensing [Li, Li, He, Chen and Plaza (2020); Chen, Huang and Xu (2015); Nguyen, Katzfuss, Cressie and Braverman (2014)], geoscience [Wu, Yin, Zeng, Duan, Göttsche, Ma, Li, Yang and Shen (2021); Ma and Kang (2020); Tang, Wang, Zhang and Atkinson (2020)], network architectures [Kashinath, Mostafa, Mustapha, Mahdin, Lim, Mahmoud, Mohammed, Al-Rimy, Fudzee and Yang (2021); Shah, Anwar, Mahmood, Tari and Zomaya (2017)], and computer vision [Duzceker, Galliani, Vogel, Speciale, Dusmanu and Pollefeys (2021); Wang, Tang, Tong and Atkinson (2020); Xue, Leung and Fung (2017)]. In the realm of computer vision, various strategies for data summarization using fusion techniques have been explored, including Gaussian entropy fusion [Fu, Guo, Zhu, Liu, Song and Zhou (2010)] and probabilistic skimlets fusion [Zhang, Gao, Hong, Hu, Ji and Dai (2014)]. Additionally, deep learning architectures have been applied for summarization tasks [Zhong, Wu and Jiang (2019)]. Notably, the proposed work takes a unique approach by leveraging information-theoretic fusion for data summarization. Unlike some existing techniques, our approach doesn't need training and can be readily applied to large-scale datasets. Moreover, it requires minimal computational costs, rendering it effective for both in situ and post hoc analysis. The feasibility of in situ application is showcased in our preliminary research [Dutta, Tasnim, Turton and Ahrens (2021)].

Information theory [Cover and Thomas (2006); Verdu (1998)] concepts such as entropy and mutual information

[Shannon (1948); Gray (2011)] have been employed to measure the relationships between variables in data across multiple computational domains [Moore, Valentini, Walker and Levin (2018); Pilkiewicz, Lemasson, Rowland, Hein, Sun, Berdahl, Mayo, Moehlis, Porfiri, Fernández-Juricic, Garnier, Bollt, Carlson, Tarampi, MacUga, Rossi and Shen (2020); Sbert, Feixas, Rigau, Chover and Viola (2022); Tasnim, Fricke, Byrum, Sotiris, Cannon and Moses (2018)]. Mutual information is extensively applied in the field of feature selection, exploration, extraction, and tracking [Biswas, Dutta, Shen and Woodring (2013); Dutta and Shen (2016); Tasnim, Dutta, Turton, Rogers and Moses (2022)]. Image registration is another popular application [Maes, Collignon, Vandermeulen, Marchal and Suetens (1997); Viola and Wells III (1997); Hill, Batchelor, Holden and Hawkes (2001); Cahill (2010)]. Mutual information, as well as its decomposition measures like specific mutual information and pointwise mutual information, have been widely used in multimodal data fusion [Bramon, Boada, Bardera, Rodríguez, Feixas, Puig and Sbert (2012)], graphics, and visualization [Wang et al. (2008); Dutta et al. (2016); Dutta, Woodring, Shen, Chen and Ahrens (2017b); Dutta, Liu, Biswas, Shen and Chen (2017a); Isola, Zoran, Krishnan and Adelson (2014); Bramon, Ruiz, Bardera, Boada, Feixas and Sbert (2013a); Akiba, Ma, Chen and Hawkes (2007); Chen, Feixas, Viola, Bardera, Shen and Sbert (2016)]. Other use cases for information theory include view selection [Viola, Feixas, Sbert and Groller (2006)], feature similarity [Bruckner and Möller (2010)], transfer function and design [Ruiz, Bardera, Boada, Viola, Feixas and Sbert (2011); Bramon, Ruiz, Bardera, Boada, Feixas and Sbert (2013b); Haidacher, Bruckner, Kanitsar and Gröller (2008)], and data sampling [Dutta, Biswas and Ahrens (2019); Wei et al. (2018)].

The works we discussed here collectively contribute to the proposed approach's design, development, and motivation. Our research draws inspiration from these methodologies and integrates information-theoretic principles to develop an innovative solution.

3. Information-Driven Framework for Feature-Based Temporal Data Summaries

3.1. Framework Workflow

In this section, we provide a comprehensive step-by-step explanation of our technique's mechanism. We intend to construct an efficient, generic, and fast data summarization workflow with minimal customization to adapt to a variety of application domains. Figure 1 illustrates the schematic of this proposed workflow. To demonstrate each step of this workflow, we will refer to Figure 2, which serves as an illustrative application of our method using a synthetic data set. In this application, we simulate a rolling ball moving 0.5 units from left to right at each timestep until it exits the view area.

Our proposed method is designed for datasets with sequence of timesteps containing various types of salient spatial features. In Figure 2, the simulated rolling ball application consists of 19 timesteps (T0 - T18), showcasing the ball's positional change over time. Each timestep is represented as 800 x 400 pixel 2D RGB images and pixel intensities ranging from 0 to 255. At timestep T0, the frame is empty; the ball has not yet entered the view area. It enters at T1 and the ball changes position until T17. In, time step T18 the ball exits the view area. The method starts with iterating over input timesteps. After the first timestep, for every subsequent timesteps, the key regions are extracted using a segmentation method proposed in [Kuruvilla, Sukumaran, Sankar and Joy (2016)]. Criteria for extraction of such key regions can be determined by the domain knowledge. In the rolling ball demonstration, the key feature is the presence of the ball and its location. So we segment the region containing the ball and create binary masked images shown in Figure 2 (masked row). These images contain only two distinct data values: 0 (no ball) and 255 (ball).

After extracting the key region, we check if a certain property is present in that timestep. We denote this property as *trigger* which is a change in the key region. The change can be in terms of count, size, shape, connectivity, space or association. In this rolling ball demonstration, the trigger is the presence of the ball in the view area. When the ball enters and exits the area, it is considered as a salient information. But the time it remains in the area, the only novel information is its change of position. If the trigger is present in the current timestep, then it is considered to be significant and a key timestep. Hence our method saves it as it is. If the trigger is not present in the current timestep, we proceed to the next timestep, do a similar check, and continue the process until a trigger event is encountered. These sequential time frames that did not have the trigger event are chosen to be fused into a single timestep as the amount of novel information within such a sequence is low. If the number of timesteps to be fused is one then we can discard it as the previous time step has the necessary information. If the number is greater than one then we perform pairwise information-guided fusion on these timestep and convert them as one single timestep to be saved as a temporal summary. Referencing the demonstration in Figure 2, T0 is saved. Then starting from timesteps T1 - T17 there is no trigger present in the timesteps. Therefore, those timesteps are fused as shown in figure 2(a) and (b). The following section sheds light on how we use information theoretic approaches for the fusion method.

3.2. Characterization of Samplewise Information for Fusion

In this work, our aim is to track and summarize the information change in fused timesteps. Therefore, we need to have a quantification of information content for each data point in the timesteps. We use the term "sample" to refer to these individual data points. Each timestep contains multiple samples representing the values of the data. For example, in the case of images like the rolling ball, these samples

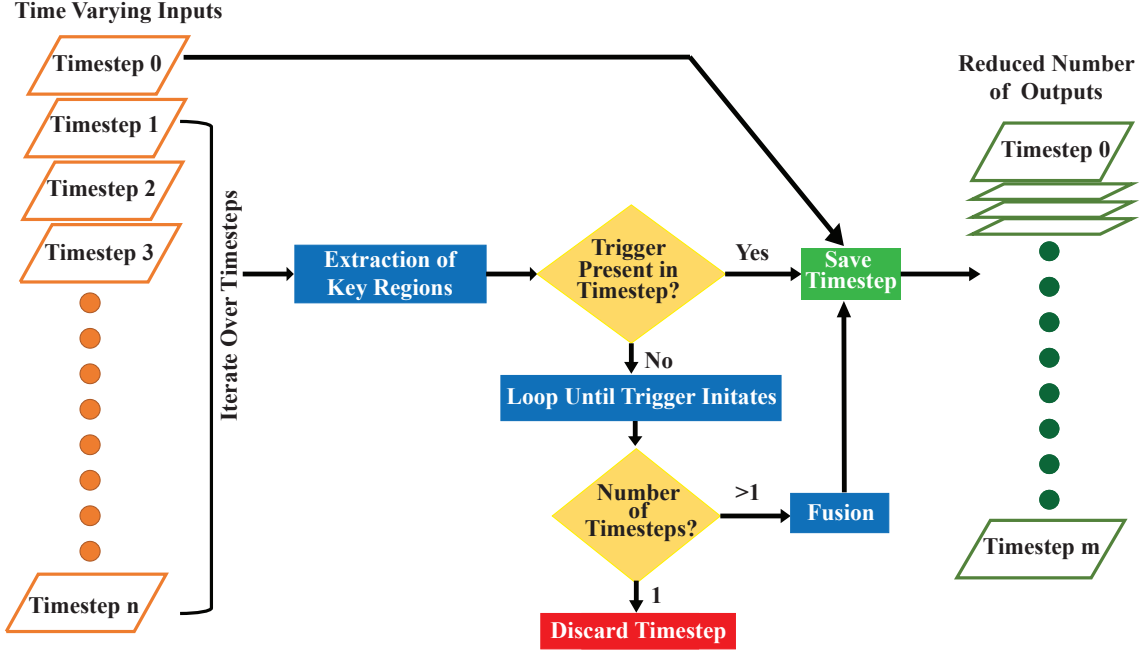


Figure 1: Schematic diagram of the workflow. We have used the standard computational flowchart [Sipser (2013)] symbols for representations: input/output, process, decision, and arrows indicating relationships between symbols.

typically range from 0 to 255, while for other types of data variables, they may be scalar values. The quantification of information for these samples will help us identify important spatial features for the timestep.

3.2.1. Mutual Informantion

In information theory, Mutual Information (MI) [Shannon (1948)] is a prominent measure that estimates the total amount of shared information between two random variables. Given two random variables X and Y , MI $I(X, Y)$ is formally defined as:

$$I(X; Y) = \sum_{y \in Y} \sum_{x \in X} p(x, y) \log \frac{p(x, y)}{p(x)p(y)} \quad (1)$$

where $p(x)$ and $p(y)$ are the probabilities of occurrence of values x for X and y for Y respectively and $p(x, y)$ is the joint probability of occurrence of values x and y together. MI assesses the degree of association or disassociation between two random variables and gives a single value. Since we aim to extract feature-based data summaries, we need samplewise spatial and temporal information characterization. Therefore, we leverage the decomposition of MI which quantifies each data value's contribution toward the association or disassociation. The decomposition of MI is termed as Specific Mutual Information or SMI [DeWeese and Meister (1999)]. SMI measures the information content of the individual scalar values of one variable (reference) when another variable (target) is observed. This information quantification helps with identifying important spatio-temporal features in the data. There are multiple methods

for MI decomposition [DeWeese and Meister (1999); Butts (2003)]. For apprehending the fusion criteria essential for summarizing the data, the properties of the SMI measure, *Surprise* holds the most potential.

3.2.2. SMI Measure Surprise

The Surprise measure denoted as I_1 was first introduced by DeWeese and Meister (1999). Surprise quantifies the information change of the target variable after observing the individual scalar values of the reference variable. The derivation of Surprise from MI is as follows.

By definition the conditional probability of x given y or $p(x|y)$ is,

$$p(x|y) = \frac{p(x, y)}{p(y)} \quad \text{or} \quad p(x, y) = p(x|y)p(y) \quad (2)$$

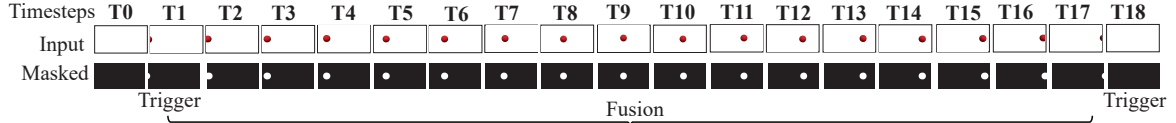
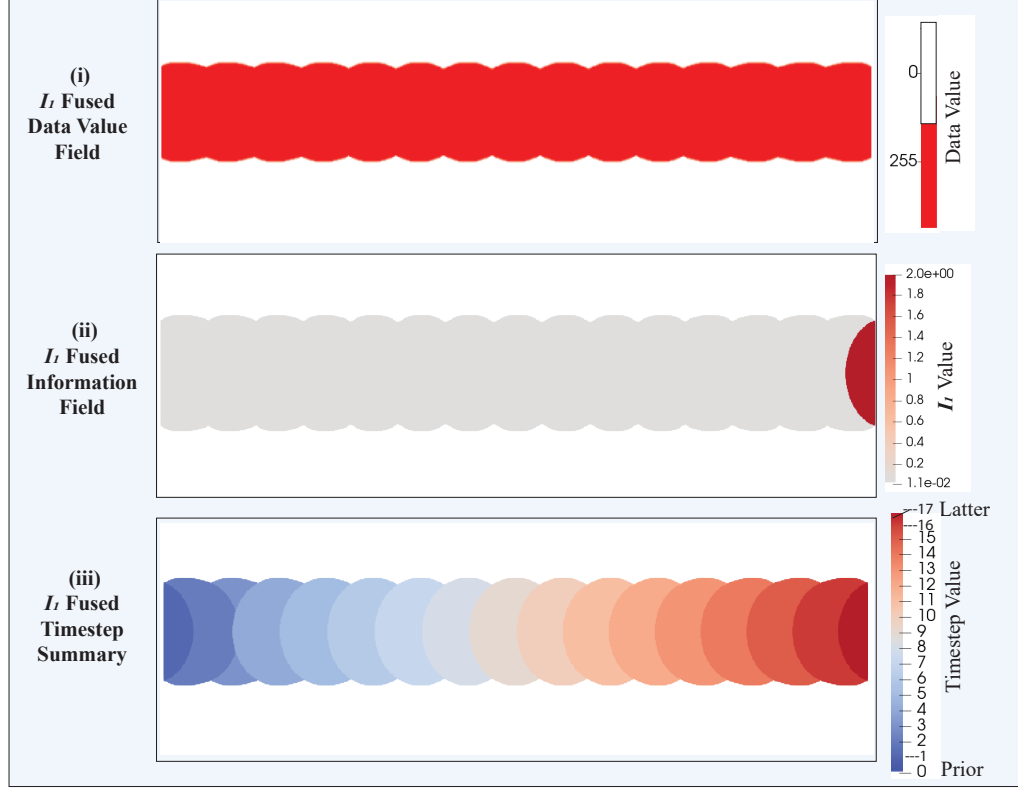
Replacing the joint probability in Equation 1, we get,

$$\begin{aligned} I(X; Y) &= \sum_{y \in Y} p(y) \sum_{x \in X} p(x|y) \log \frac{p(x|y)}{p(x)} \\ &= \sum_{y \in Y} p(y) I_1(y; X) \end{aligned} \quad (3)$$

where,

$$I_1(y; X) = \sum_{x \in X} p(x|y) \log \frac{p(x|y)}{p(x)} \quad (4)$$

Equation 4 represents the surprise measure of data value y from Y after observing all the values of X . A high value


 (a) Surprise (I_1) Guided Fusion


(b) Pointwise Mutual Information (PMI) Guided Fusion

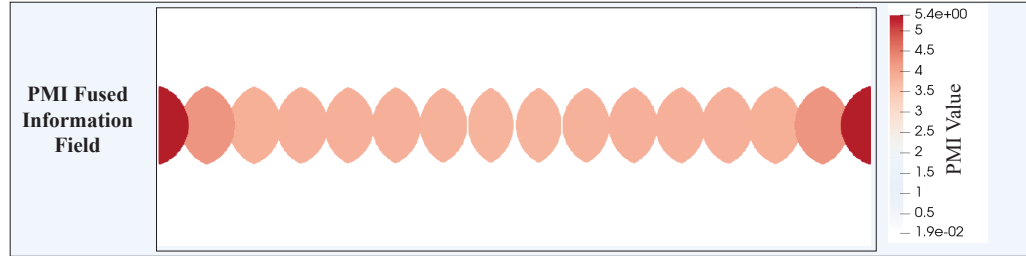


Figure 2: Illustration of a simulated rolling ball with 19 timesteps (T0 -T18). At each timestep, the ball moves 0.5 units to the right. Timesteps are 2D RGB images with 800×400 dimensions and samples ranging from 0 to 255 (input row). The masked row presents binary images with values 0 (no ball) and 255 (ball) after ball segmentation. Timesteps T1 to T17 are fused using (a) Surprise (I_1) guided fusion and (b) PMI guided fusion. a(i) shows the I_1 fused data value field of the fused timesteps(0 white and 255 red). a(ii) shows I_1 fused information value field. a(iii) displays I_1 fused timestep summary with numbered color labels for each timestep. The numbers indicate spatial information changes over time. Surprise effectively captures spatio-temporal properties, whereas alternative measure PMI does not perform as well. (b) presents the scenario with the information field with PMI values

for $I_1(y; X)$ means after observing y , some previously low probable values of $x \in X$ have become highly probable in the distribution. This likelihood increase is the element of surprise and a salient finding for further analysis. Surprise is also the only positive decomposition of MI since it is the Kullback-Leibler distance between $p(x|y)$ and $p(x)$ [Kullback and Leibler (1951)]. In the fusion process of the data

summarization, the data samples with high surprise values stand out and are identified as important features.

3.3. Surprise (I_1) Guided Fusion Technique

When the low informative timesteps are chosen, the fusion initiates for summarization. The fusion is done on pairwise timesteps. For every pair of data samples from the

timesteps, we store samples contributing to more information or high I_1 values. This fusion strategy was introduced in [Bramon et al. (2012)] for fusing different datasets to gain the most informative combination. The condition to compute the fused value using I_1 -fusion is:

For every data sample pair with (x, y) , the fused value, f is,

$$f = \begin{cases} x, & \text{if } I_1(x; Y) > I_1(y; X) \\ y, & \text{otherwise} \end{cases} \quad (5)$$

Here $x \in X$ and $y \in Y$ are individual data values from two data sets X and Y respectively. Our fusion criteria is based on the idea of Equation 5, however, instead of different datasets we are using two subsequent timesteps from the same dataset. To fuse multiple timesteps, we begin by creating a fused timestep using the first two timesteps. Then, we repeat the fusion process by comparing the fused timestep with the next timestep, and continue until all desired timesteps have been fused. Our strategy involves updating the fused timestep during each iteration and selecting the spatial and temporal values with the highest information content. By the end of the process, the resulting fused timestep will represent a summary capturing their most informative properties with direction. The fusion process is described in detail in Algorithm 1. After each fusion process, the algorithm provides 3 fused fields as shown in 2(a). I_1 fused data value field contains the values of the data samples with high surprise measure. I_1 fused information value field contains the I_1 values for the same sample positions. In the timestep summary fields, the same data sample are labeled with their originating timestep numbers.

Applying the fusion process in Algorithm 1 on the timesteps T1 - T17 of the simulated rolling ball, the surprise (I_1) fused data value field is generated highlighting the path of the rolling ball with data values 255 as shown in Figure 2 a(i). The regions without the ball are valued 0 or white. Figure 2 a(ii) represents the fused information fields with I_1 values. From the color bar's gradient, we observe that the surprise values exhibit limited variation, spanning approximately from 0 to 2. A minimal data value range results in minimal surprise value variation. Figure 2 a(iii) presents the timestep summary where the numbers of originating timesteps are labeled for the salient samples. Here, we employed distinct colors to label the timesteps, enabling clear visualization and differentiation of each timestep. This color-coded representation effectively showcases the flow of information, facilitating the tracking of information changes over time. Here, the confidence threshold is employed to downplay the non-important regions. In this particular case, the threshold value is set to 255. Any value below 255, representing the absence of the ball, is assigned as timestep 0. In Figure 2 a(iii), these regions are depicted as white or transparent (steps 19 - 24 in Algorithm 1). The method reduces the number of output timesteps from 19 to 3 in the simulated rolling ball case, achieving substantial data reduction with minimal information loss. The fused timestep

effectively visualizes the information changes over time, serving as a concise summary of the original data dynamics.

Algorithm 1 Fusion Process

Input:

- data1: Array of data values from fused timestep. Initialized with the first timestep.
- data2: Array of data values from the subsequent timestep.
- Ifield1: Array of I_1 values for $I_1(x; Y) \forall x \in X$
- Ifield2: Array of I_1 values for $I_1(y; X) \forall y \in Y$
- timestep_fuse: Array of timestep values. Starts with 0
- time: Current timestep value
- conf_th: Confidence threshold for the key regions.

Output:

- fused_field_data: Array of the fused data values
- fused_field_I1: Array of the fused I_1 values
- timestep_fuse: Array of the fused timestep values.

```

1: procedure CREATEFUSIONFIELDS(data1, data2,
   Ifield1, Ifield2, timestep_fuse, time, conf_th)
2:   fused_field_data  $\leftarrow$  array of zeros with shape data1
3:   fused_field_I1  $\leftarrow$  array of zeros with shape data1
4:   for i  $\leftarrow$  0 to data1.shape[0] - 1 do
5:     for j  $\leftarrow$  0 to data1.shape[1] - 1 do
6:       if Ifield1[i][j] > Ifield2[i][j] then
7:         fused_field_data[i][j]  $\leftarrow$  data1[i][j]
8:         fused_field_I1[i][j]  $\leftarrow$  Ifield1[i][j]
9:         if time = 1 then
10:           timestep_fuse[i][j]  $\leftarrow$  time
11:         end if
12:       else
13:         fused_field_data[i][j]  $\leftarrow$  data2[i][j]
14:         fused_field_I1[i][j]  $\leftarrow$  Ifield2[i][j]
15:         timestep_fuse[i][j]  $\leftarrow$  time + 1
16:       end if
17:     end for
18:   end for
19:   for i  $\leftarrow$  0 to data1.shape[0] - 1 do
20:     for j  $\leftarrow$  0 to data1.shape[1] - 1 do
21:       if fused_field_data[i][j] < / > conf_th then
22:         timestep_fuse[i][j]  $\leftarrow$  0
23:       end if
24:     end for
25:   end for
26:   return fused_field_data, fused_field_I1, timestep_fuse
27: end procedure

```

3.4. Alternative Fusion Approaches

The measure Surprise effectively apprehends the spatio-temporal features for the data summarization process. However, we also explore several other potential information measures to devise alternative techniques for generating data summaries. These information-theoretic measures include Pointwise Mutual Information (PMI) [Church and Hanks (1990)], SMI measure (1) predictability (I_2) [DeWeese and

Meister (1999)] and (2) *stimulus* specific information (I_3) [Butts (2003)]. These measures were investigated because they are the decomposition of MI and they possess the ability to analyze the contributions of individual data values in quantifying the information content of spatio-temporal data. They offer insights into the properties of data samples concerning information analysis.

3.4.1. PMI Guided Fusion

Pointwise Mutual Information (PMI) [Church and Hanks (1990)] quantifies the degree of association (or disassociation) between individual data points given two variables. If X and Y are two variables, then each data point can be represented by the value pair (x, y) where $x \in X$ and $y \in Y$. The statistical association between these two points can be measured by their PMI value, which is formally expressed as:

$$\text{PMI}(x, y) = \log \frac{p(x, y)}{p(x)p(y)} \quad (6)$$

where $p(x)$ and $p(y)$ are the probabilities of occurrence of values $x \in X$ and $y \in Y$ respectively, and $p(x, y)$ is the joint probability of occurrence of values x and y together. PMI was introduced by Church and Hanks (1990). Comparing Equations 1 and 6, we can infer that the expected PMI values over all occurrences of variables X and Y correspond to the mutual information value $I(X; Y)$. PMI is a symmetric measure that can generate values ranging from negative to positive, depending on whether the distributions are complementary or overlapping. If the information overlap is high ($p(x, y) > p(x)p(y)$), then $\text{PMI}(x, y) > 0$. The low association is indicated by $p(x, y) < p(x)p(y)$, resulting in $\text{PMI}(x, y) < 0$. If x and y are statistically independent then $p(x, y) = p(x)p(y)$ and $\text{PMI}(x, y) = 0$.

Now, given the PMI measure, we can devise a fusion strategy similar to I_1 where I_1 values are substituted with PMI values in Algorithm 1. The resulting fused information field on the simulated rolling ball is shown in Figure 2(b). We observe that PMI fails to capture the spatial characteristics of the key regions and only captures the overlapped regions that are strongly associative, indicated by high positive PMI values. The non-overlapping regions are transparent showing low information overlap. The PMI values here are 0 meaning data distribution is complementary and statistically independent. As the spatial position of sample pairs plays a critical role in PMI calculation, the fused field properties can exhibit significant variation depending on the degree of overlap between the key features.

3.4.2. I_2 Guided Fusion

Predictability (I_2) is another decomposition of MI introduced by DeWeese and Meister (1999). This SMI measure quantifies the change in the uncertainty of one variable (X) after observing the individual value of another variable ($y \in Y$) and is computed as:

$$I_2(y; X) = - \sum_{x \in X} p(x) \log p(x) + \sum_{x \in X} p(x|y) \log p(x|y) \quad (7)$$

where $y \in Y$ is the reference variable and $x \in X$ is the target variable. $p(x)$ is the probabilities of occurrence of values x for X and $p(x|y)$ is the conditional probabilities values x given values y . Upon observing the variable y , the uncertainty of variable X can either increase or decrease, leading to the possibility of both positive and negative values for the I_2 measure. In some cases, the increased uncertainty can reveal significant information about the relationship between the variables. However, when we use the I_2 measure instead of the I_1 measure in the fusion process, the resulting fused information does not offer a meaningful summary over time. This measure intermittently highlights notable information changes, failing to capture the overall data dynamics. Our hypothesis is that this measure is more suitable for feature extraction and uncertainty quantification across various datasets rather than for analyzing consecutive timesteps within a single dataset.

3.4.3. I_3 Guided Fusion

There is another measure that is derived from the decomposition of MI and was introduced for measuring the association of stimulus and response in certain neural systems [Butts (2003)]. It is termed as Stimulus Specific Information (SSI), denoted by I_3 and computed as:

$$I_3(y; X) = - \sum_{x \in X} p(x|y) I_2(x; Y) \quad (8)$$

The response and stimulus are the two variables X and Y . This measure focuses on establishing the association between the two variables to extract the maximum amount of information from their relationship. It emphasizes that the most informative data values from the first variable are related to the most informative data values of the second variable [Butts (2003)]. In some cases, I_1 can be an alternate measure for I_3 , but the interpretation is different based on the data [Butts (2003)]. They both capture different properties in the data. When we use the I_3 measure instead of the I_1 measure on the simulated rolling ball dataset, it captured very similar properties shown in Figure 2(a). However, when applied to a different and more complex dataset, it failed to capture the spatial properties of the features in the summarization. This is explained in detail in Section 4.1.2 and shown in Figure 3(b).

From the various methods mentioned, it's clear that different approaches emphasize distinct data properties. After thorough investigation of various information-theoretic methods, we found that the Surprise measure aligns best with our objectives of highlighting features and summarizing spatio-temporal data while tracking information flow. In the next section, we apply this method to more complex datasets to demonstrate its versatility across different data scenarios.

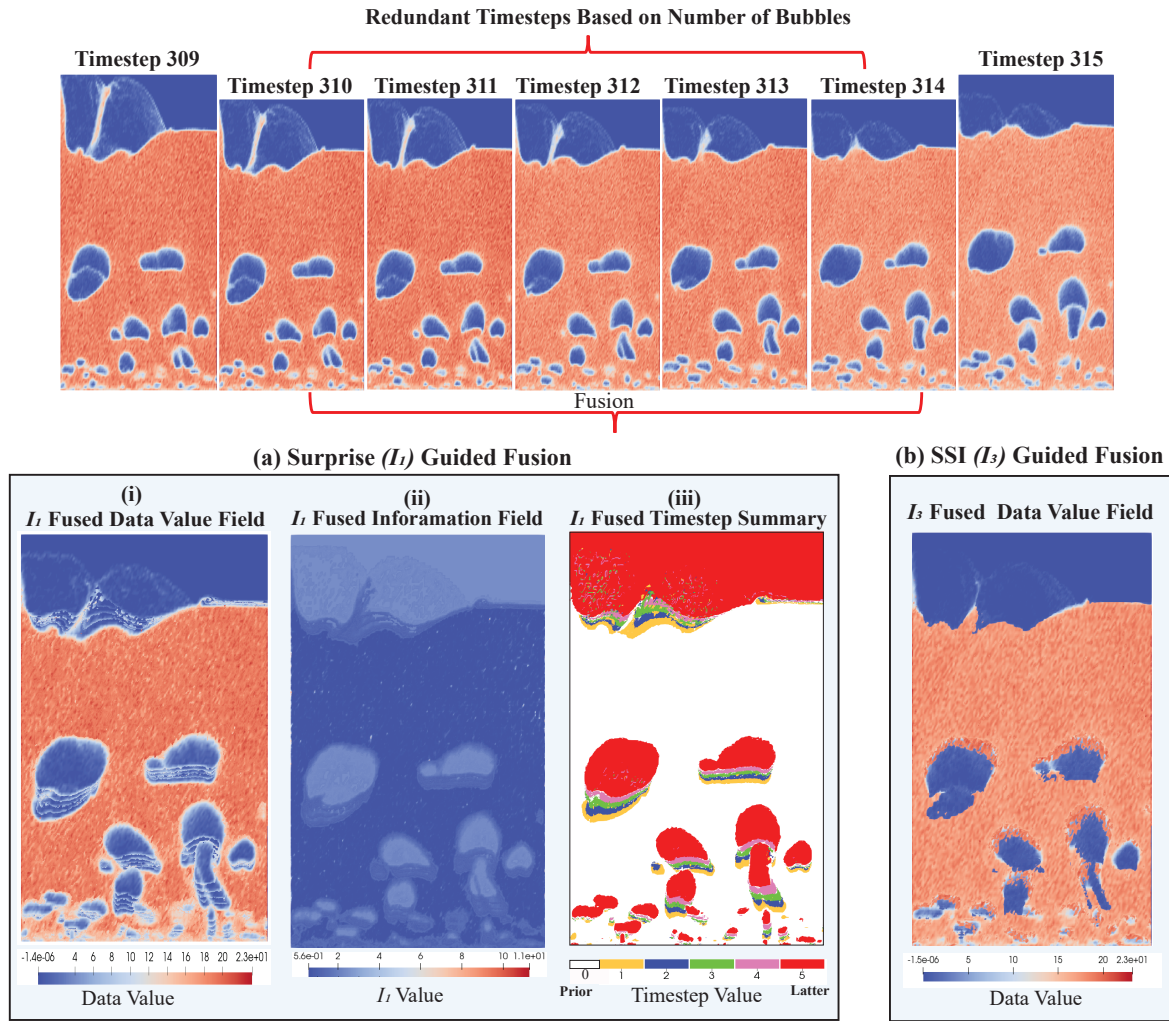


Figure 3: Analysis and illustration of dynamic spatio-temporal summarization for MFIX-Exa simulation application. The first row represents multiple timesteps (309 - 315) of the dataset where the bubbles are highlighted as the blue regions. Timesteps are raw images with 488×842 dimensions. Timesteps 310 to 314 are fused using (a) Surprise (I_1) guided fusion (i-iii) and alternative (b) Stimulus Specific Information (SSI) or I_3 guided fusion. a(i) shows the I_1 fused data value field of the timesteps, a(ii) shows I_1 fused information value field reflecting I_1 values and (c) shows I_1 5 fused timestep summary. The color bar labels 5 different colors summarizing the flow and direction of the bubbles in one timestep. The alternative I_3 is unable to capture the path of bubbles as reflected in (b) I_3 fused data field.

4. Applications

In this section, we assess the versatility of our DSTS method across various multidisciplinary applications, demonstrating its effectiveness in handling complex and diverse datasets with streaming characteristics.

We selected diverse applications across multiple domains to demonstrate the method's robustness. The first dataset involves multiphase flow simulation with scalar data values. The second is a surveillance video with extended timesteps to highlight optimization capabilities. The third dataset comprises complex immune cell images. This comprehensive evaluation showcases the method's adaptability and utility across various research disciplines.

4.1. MFIX-Exa Flow Simulation

MFIX-Exa [Musser, Almgren, Fullmer, Antepará, Bell, Blaschke, Gott, Myers, Porcu, Rangarajan, Rosso, Zhang and Syamlal (2022)] is a particle-based multiphase flow simulation developed by the National Energy Technology Laboratory (NETL), USA. It focuses on modeling multiphase flow by interacting with a vast number of particles within the simulation domain. Using MFIX-Exa, particle-based data is generated for studying the operational principles of chemical looping reactors (CLR). MFIX-Exa can simulate various chemical mixing processes and one such simulation involves the interaction of carbon particles with air in a fluidized bed, resulting in the formation of carbon dioxide bubbles or void regions. These bubbles hold significant importance

for domain experts. MFIX-Exa generates vast data with numerous particles and thousands of timesteps. This extensive raw data presents challenges in transferring to storage due to limited I/O bandwidth. Hence, experts seek solutions to extract bubble-specific information while reducing storage needs, and preserving temporal bubble dynamics. Our proposed dynamic spatio-temporal summarization method can be used to provide this solution.

4.1.1. Data Context and Features

The raw data of the MFIX-Exa simulation contains the value of particle properties (i.e., position, velocity, momentum, etc.) over multiple time steps. As the data is streaming in nature, therefore it is a good fit for our proposed workflow. In Biswas, Ahrens, Dutta, Musser, Almgren and Turton (2021), there is a detailed description of how this streaming simulation is converted into a 3D scalar dataset.

For this work, we use 2D slices extracted from this raw 3D scalar data. These slices contain scalar values representing particle density. As a result, our dataset consists of multiple timesteps (count 332), and each timestep corresponds to 2D data samples with dimensions of 488 x 842. The sample values fall within the range of $[-1.2 \times 10^{-6}, 29.08]$. As mentioned earlier, the key regions are the **bubbles**. The bubbles are the low particle density regions. In Dutta, Turton, Rogers, Musser, Ahrens and Almgren (2022), the detection, segmentation, and characterization of the bubbles are developed and studied in an extensive manner. Using a density threshold, the bubbles are segmented. Then, the VTK [Schroeder, Martin and Lorensen (1998)] library is used to extract the connected components in the dataset and use the threshold value to filter the low-density bubbles. Over time, the bubbles undergo phases like creation, merge, split, and dissolve into air [Biswas et al. (2021)]. Using data from this simulation, domain experts want to comprehend the evolution of bubbles and explore the relationships between various bubble characteristics such as their size, shape, number of bubbles, etc [Dutta et al. (2022)]. Important events in this simulation can be characterized by the creation of a bubble, the merging of two or more bubbles, or the dissolving of a bubble. Note that for all of these events, the total number of bubbles will change. Hence, if we identify time steps when the bubble number has changed from a previous time step, then that can be considered as a "trigger". In this work, we skip counting changes in very small bubbles for simplicity. Key time steps are saved when the trigger occurs, and intermediate steps between two triggers are fused using Algorithm 1 to summarize and store them. This process continues for all timesteps.

4.1.2. Results for Data Summarization

Figure 3 shows the analysis of DSTS method for MFIX-Exa simulation. Timesteps 309 - 315 are shown in the first row where bubbles are the blue regions. From 311 to 314 the number of bubbles remains unchanged. Therefore timesteps 310 - 314 are summarized using the fusion process. Figures 3 (a) represent results from the Surprise I_1 guided fusion. The

I_1 fused data value field a(i) shows the scalar values $[-1.4 \times 10^{-6}$ to 23] for the fused timesteps. Here the change in bubble movement is very prominent. Figure 3 a(ii) presents the I_1 values $[5.6 \times 10^{-1}$ to 11] for the fused timesteps. The range of information value (I_1) is smaller, making it less sensitive to bubble movement compared to particle density values. However, it effectively highlights the main bubbles and their temporal dynamics. The timestep summary field depicted in Figure 3 a(iii) represents the timestep values from which the bubbles originate. Here 5 timesteps are color-coded in distinguished colors to highlight the flow of the information between interacting bubbles. The color map reflects the direction of the bubbles from the start to the end position. This summary field not only emphasizes key features but also visually indicates the spatial information flow over time. The white/ transparent background (labeled as 0) filters all the density values that are of low importance for this dataset.

We also implemented the alternative SSI (I_3) guided fusion technique as mentioned in Section 3.4.3 for MFIX-Exa. Figure 3(b), represents the I_3 fused data value field. Here the bubbles are somewhat highlighted but the change in the bubbles' movement is hard to interpret. I_3 captures some spatial features of the bubble regions but the edges are blurred. Thus, the surprise fusion method again proves to be better than the SSI measure.

Based on the outcomes observed in both the simulated rolling ball and MFIX-Exa simulation applications, it is evident that the timestep summary field stands out as the most informative visual representation for spatio-temporal summarization. This representation encapsulates both spatial and temporal dynamics by highlighting the key regions and indicating the direction of the information flow over time. Consequently, for our analysis of the next two applications, we only show the surprise fused **timestep summary fields**.

4.2. Surveillance Data Analysis and Optimization

Data summarization techniques are vital for security camera footage analysis. Security camera systems generate vast amounts of data, and manually reviewing the continuous stream of video can be time-consuming and laborious. DSTS offers an efficient solution by allowing the analysis and optimization of camera footage. Suspicious activities can be detected by choosing an appropriate "trigger" and the generated summary fields provide experts with an intuitive visual representation of the key timesteps. The most significant impact of our method in this application is on archiving and storage optimization.

To demonstrate DSTS in security camera footage analysis, we used the publicly available SBM-RGBD Dataset [SBM-RGBD Dataset; Camplani, Maddalena, Moyá Alcover, Petrosino and Salgado (2017)]. This dataset was originally created in conjunction with the Workshop on Background Learning for Detection and Tracking from RGBD Videos [RGBD2017]. It was created to evaluate background modeling methods for moving object detection. The dataset comprises 33 RGBD videos, totaling 15033

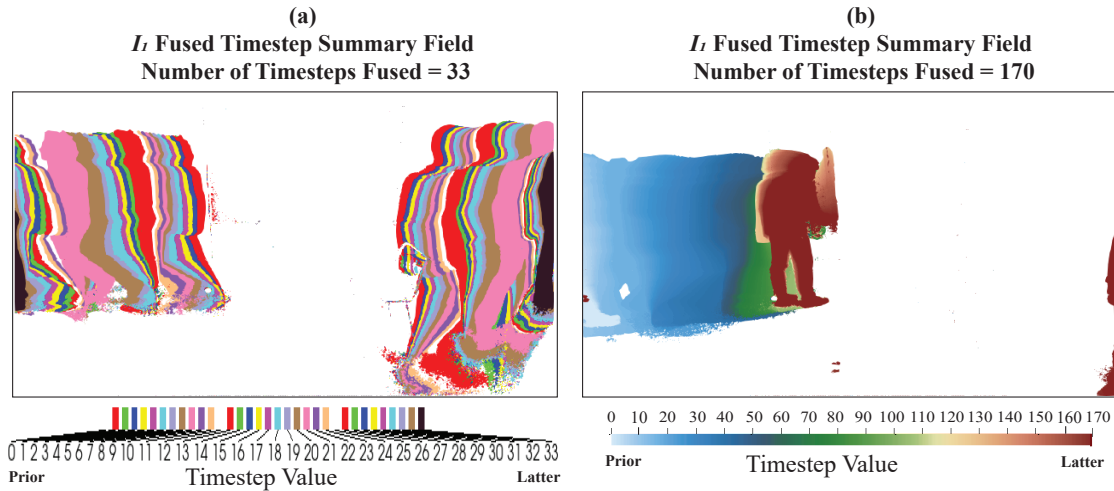


Figure 4: Analysis and illustration of the dynamic spatio-temporal summarization for the SBM-RGBD dataset. Here the emphasis is on representing the extensive number of timestep summaries. (a) shows a summarization of 33 fused timesteps using a discrete color bar to illustrate information changes over time. (b) showcases a summarization of 170 fused timesteps, employing a continuous flow color bar to depict information changes over a longer period. The color bars point out the spatial direction of the information flow by denoting the prior and latter states.

timesteps, recorded indoors using a Microsoft Kinect sensor [Camplani et al. (2017)]. The dataset contains videos capturing moving objects at intervals, which aligns with the data requirements for our application. Here, we used one of the videos titled "Multiple2" which shows four individuals walking in and out of the view area, engaging in discussions, and writing on a whiteboard. Our method shows an effective demonstration of summarizing the movement patterns of the individuals.

4.2.1. Data Context and features

The videos have 640 x 480 resolution and the length is 1400 timesteps. The dataset comes with image (PNG) files for each timestep of the input video. We recreated the videos from the images which can be visualized here [BC lab ref]. The key regions in this dataset are the individuals and their movement. The whiteboard and a chair are stationary in the background. To extract key regions from the background, we have used a method called ViBe: a universal background subtraction algorithm designed for video sequences [Barnich and Van Droogenbroeck (2010)]. The algorithm aims to identify moving objects within consecutive images or videos by efficiently distinguishing between the foreground (moving objects) and the background (stationary elements). The algorithm is computationally lightweight, making it suitable for real-time applications. The adaptability of ViBe has made it a popular choice for a range of computer vision tasks, including object tracking, surveillance, and motion detection. Its straightforward pseudocode provided in Barnich and Van Droogenbroeck (2010) facilitates easy implementation. By applying the ViBe algorithm, the RGB images are converted into masked binary images with segmented individuals in the foreground.

In scenarios with multiple individuals in the frame, we adopt a concept similar to that used for counting bubbles in the MFIX-Exa (Section 4.1). We apply the concept to count the number of people in each timestep by analyzing the largest connected regions in the masked images. Since it is a binary image, the data samples have two values: 0 (no individual) and 255 (individual). By setting a size threshold, we can accurately count the number of individuals in each timestep. Given that individuals move in and out of the view area in the dataset, the number of individuals can be used as a trigger for our application. Whenever a person enters or exits, that is a key timestep. The consecutive timesteps between two triggers are then fused using Algorithm 1. This fusion process effectively summarizes the movement patterns of individuals within one timestep, eliminating the need to store every less informative timestep.

The combination of the key and summary timesteps, provides an intuitive visual representation of the significant moments in the video, making the analysis of surveillance scenarios more informative.

4.2.2. Results for Data Summarization

Figure 4 showcases the summarization fields for two separate fused timesteps in the dataset. Both fields show Surprise(I_1) fused timestep summaries, effectively representing spatial features and movement directions of individuals over time. In this particular application, our main aim is to showcase how effectively the method can fuse longer timesteps while ensuring that both spatial and temporal dynamics remain just as noticeable as they are in shorter timesteps.

In Figure 4(a), the summarization field depicts a fusion of 33 timesteps, where two individuals are walking out of the view area. The leftmost person exits first, initiating the

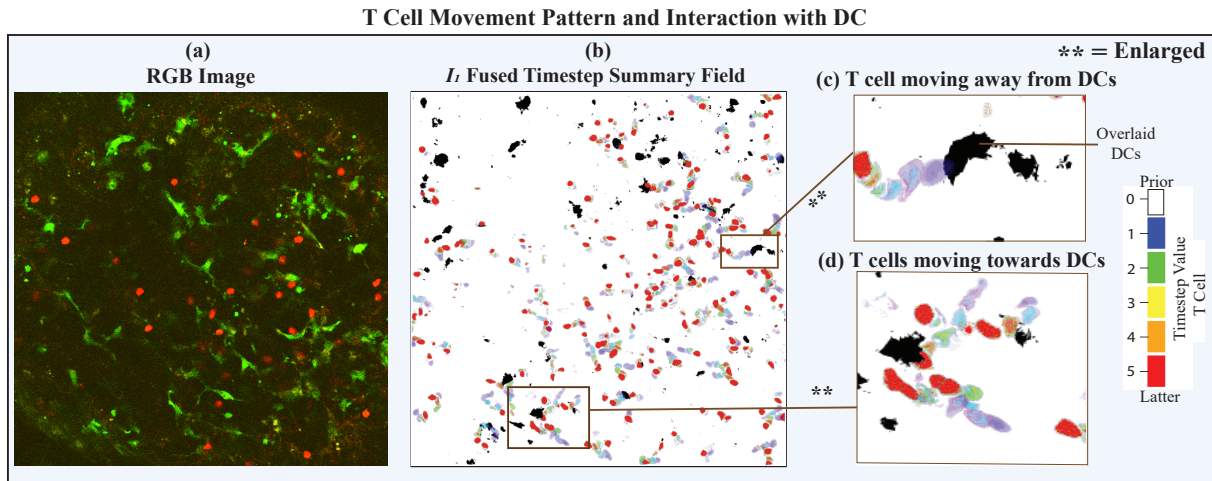


Figure 5: Illustration and analysis of the dynamic spatio-temporal summarization method for cell interaction in Lymph Node. The results emphasize T cell movement patterns and interaction with DCs in LN. (a) is a sample timestep. Here red indicates the T cells and green indicates the DCs. (b) is the surprise fused timestep summary fields of T cell for 5 timesteps. The black cells in the field are overlaid DCs to highlight cell contact. (c) and (d) are 2 enlarged positions from the (b) field to emphasize T cell movement. (c) shows that a T cell is moving away from the DCs. (d) shows multiple T cells moving toward the DCs. The corresponding timestep values are provided in the color bars to highlight the direction.

trigger and stopping the fusion process. Each timestep is represented by a discrete color, highlighting the changes in movement over the 33 timesteps. Sample values below 255 are set to 0, representing the white background, as the data value of individuals is 255.

Figure 4(b) shows a timestep summary for a longer period of 170 timesteps. The summarization field captures an individual walking into the view area and writing on the board, while another person has just stepped in, initiating the trigger event. Continuous colors are used to display the movement changes due to the length of the fused timesteps.

Remarkably, key and summarized timesteps in this dataset result in a significant reduction from 1400 timesteps to only 49 timesteps. The highest number of timesteps being fused is 262. This notable optimization ensures that only relevant information is stored, reducing storage requirements without compromising critical insights into the movement patterns of individuals. By efficiently identifying and storing key moments, our method enhances the analysis of crowded environments, enabling rapid detection of suspicious activities, and thereby serving as a valuable tool for surveillance.

4.3. Tracking Cell Interactions in Lymph Nodes

This dataset contains consecutive images of cellular interactions within the lymph node (LN). LNs are essential for immune function, playing a crucial role in initiating immune response and facilitating immune cell communication [Mirsky, Miller, Linderman and Kirschner (2011)]. In the LN micro-environment, naive T cells are activated by interactions with different cell types. Understanding these interactions provides valuable insights into immune activation [Brewitz, Eickhoff, Dähling, Quast, Bedoui, Kroczeck, Kurts, Garbi, Barchet, Iannacone et al. (2017)]. We reanalyze data from [Tasnim et al. (2018)] where information theory-based

approaches were used to identify and quantify the spatial relationships between naïve T cells and three target cellular components: dendritic cells (DCs), fibroblastic reticular cells (FRCs), and blood vessels (BVs). These interactions are critical in influencing T cell movement and the timing of encounters with antigen-presenting DCs. This process is a key step in T cell activation and the initiation of the adaptive immune response.

The data for the study was gathered using two-photon microscopy (2PM) [Rubart (2004)] to acquire 3D image stacks of lymph node tissue samples from mice. The imaging process captured dynamic movies lasting 10 to 45 minutes, resulting in a sequence of 3D images over time. This dataset is well-suited for the application of our method.

In the following sections, we demonstrate that our approach offers both quantitative analysis and visualization of cell movement and communication. Additionally, this dataset showcases the extension of our technique's applicability to 3D images and movies, highlighting its versatility and suitability for complex spatial interactions in biological systems.

4.3.1. Data Context and Features

Figure 5(a) shows 2 RGB 3D images with T cells dyed red and Dendritic Cells dyed green. Each voxel contains the color intensities of the dye in the red, blue, and green channels. For every time step, we extract the red and green channels into two separate images. We focus on the red channel in order to analyze T-cell motility.

Because these images contain a lot of noise, we implemented a pre-processing step using the median filter [Gonzales and Wintz (1987)], to reduce noise while preserving the edges of the cells for improved visualization. Since the red

channels specifically represent the T cells we did not need to segment the data.

Our goal is to visualize how T cells move and interact in these movies. In [Tasnim et al. (2018)] we used mutual information (MI) and normalized mutual information (NMI) to quantify associations between cells. Here for each timestep, we use the MI value between two cell types as a "trigger" for fusing time steps. If the MI value for a specific timestep exceeds a specified threshold, we save that as key timestep. If the MI value falls below the threshold, we find the next timestep in which the MI value exceeds the trigger threshold and fuse the intermediate ones. This allows us to efficiently capture and represent significant interactions while fusing less informative time steps. This provides an informative summary of T cell interactions within the dataset.

4.3.2. Results of Data Summarization

Figure 5 focuses on the T cell movement pattern and interaction with DCs in the summarized timesteps. Figure 5(a) is a sample timestep of T:DC dataset with 512 x 512 x 22 dimensions. This dataset has total 51 timesteps. Figure 5(b) displays the Surprise (I_1) fused timestep summary field, representing five fused timesteps from this dataset. The black cells in the summarization represent the Dendritic cells' value field overlaid on the fused summary field, visually illustrating the physical interactions between T cells and antigen-presenting DCs. Given that there are multiple interactions captured in each timestep, we highlight two specific interactions by enlarging the locations in Figures 5(c) and (d). In Figure 5(c), we observe a T cell moving away from the DCs. The color bar on the right side indicates the first (blue) and last (red) timesteps in the summary field, clearly indicating the movement direction. In Figure 5(d), we see multiple T cells moving toward the Dendritic cells, with cells making explicit contact with the DCs. The visualization provided by the fused timestep summary field allows for a comprehensive understanding of the dynamic interactions between T cells and DCs, providing valuable insights into the temporal dynamics of immune cell communication.

Our method, successfully visualizes physical contact between cells and track movement over time. Other studies [Dunn, Kamocka and McDonald (2011); Mrass, Oruganti, Fricke, Tafoya, Byrum, Yang, Hamilton, Miller, Moses and Cannon (2017); Mempel, Henrickson and Von Andrian (2004)] using similar datasets have presented the statistical quantification of association. This addition of the visualization feature has the potential to unveil more insights for experts to analyze these associations for further investigation. This is a notable contribution to the study of T cell motility, a crucial aspect for understanding immune response dynamics.

5. Discussion

The proposed DSTS technique has demonstrated its effectiveness and versatility across various applications. Starting with a simple simulation of a rolling ball to analyzing complex cellular interactions within lymph nodes, the

method proved its robustness for every application scenario. The combination of the key and fused timestep resulting from the method provides an impactful data summarization. The intuitive visual representation is a plus in showcasing an ideal blend of data optimization while preserving vital information change over time. We investigated multiple information theory measures and established that SMI measure surprise has the ability to capture the spatio-temporal features effectively.

We selected applications from multiple domains to shed light on different aspects of the DSTS method. This technique offers a practical solution to downsample and analyze the vast particle data (bubbles) generated by the MFiX-Exa simulation. This application analysis focuses on the fact that the method is able to handle scalar value data as well as image data that incorporates the rest of the applications.

The RGBD tracking dataset was introduced to show the method's ability to summarize and highlight important movement patterns of individuals for longer periods of time. The results from this dataset reflect that longer fused timesteps are equally apprehensible as the shorter timesteps. This has promising implications for surveillance and security applications, enabling more efficient and informative analysis of large video datasets.

We increased the complexity of the dataset gradually to prove the method's scalability. The T cell and Dendritic cell interactions in lymph nodes is a complex dataset. T cells which are the key regions were ample in number and the interactions with DCs were sporadic in nature. Given the fact that there were multiple interactions, our method was able to track every one of them. The summarization highlighted immune cell communication by providing a clear and comprehensive visualization of the T cell movement. The cell interaction visualization opens up new possibilities for immunological research.

All the applications in this work present post hoc data analysis. The datasets were already available when the method was applied. Since the method is not computationally expensive it can be easily combined as a step for analyzing data when they are generated; which is termed as in situ analysis. Through the integration of this method in any situ analysis, the resulting data will be optimized in real-time ensuring storage reduction with minimal data loss.

6. Conclusion and Future Work

While the method's performance on these datasets is very promising, challenges may arise in selecting appropriate triggers and threshold values, especially in complex datasets with multiple key features, interactions, and noise. However, the flexibility of the technique allows for the adjustment of parameters to tailor the summarization process to different applications. Additionally, future research could explore combining different information-theoretic measures to further enhance the summarization capabilities and address specific challenges in various datasets.

In conclusion, the proposed dynamic spatio-temporal summarization technique offers a powerful and efficient tool for visualizing and analyzing complex time-varying datasets across different domains. The method has demonstrated its adaptability and potential to provide valuable insights and understanding of temporal data dynamics. The approach holds promise for advancing research in various fields which may lead to novel discoveries and applications, ultimately contributing to a deeper understanding of complex data systems.

CRedit authorship contribution statement

Humayra Tasnim: Conceptualization, Methodology, Software, Data curation, Validation, Visualization, Writing - Original draft preparation, Writing - review and editing .
Soumya Dutta: Conceptualization, Supervision, Methodology, Validation, Writing - Original draft preparation, Writing - review and editing.
Melanie Moses: Supervision, Writing - review and editing.

Declaration of Competing Interest

The authors declare that they have no known competing financial interests or personal relationships that could have appeared to influence the work reported in this paper.

Data Availability

Data will be available upon request to the corresponding author.

Acknowledgements

We thank Judy Cannon for providing the biological data; Matthew Fricke for help on the cell interaction and analysis; Moses Biocomputational Lab at UNM for helpful discussion; IIT Kanpur.

References

- Ahrens, J., Jourdain, S., O'Leary, P., Patchett, J., Rogers, D.H., Petersen, M., 2014. An Image-Based Approach to Extreme Scale in Situ Visualization and Analysis. International Conference for High Performance Computing, Networking, Storage and Analysis, SC 2015-Janua, 424–434. doi:10.1109/SC.2014.40.
- Akiba, H., Fout, N., Ma, K.L., 2006. Simultaneous classification of time-varying volume data based on the time histogram., in: EuroVis, pp. 1–8.
- Akiba, H., Ma, K.L., Chen, J.H., Hawkes, E.R., 2007. Visualizing multivariate volume data from turbulent combustion simulations. Computing in Science and Engineering 9, 76–83. doi:10.1109/MCSE.2007.42.
- Barnich, O., Van Droogenbroeck, M., 2010. Vibe: A universal background subtraction algorithm for video sequences. IEEE Transactions on Image processing 20, 1709–1724.
- Biswas, A., Ahrens, J.P., Dutta, S., Musser, J.M., Almgren, A.S., Turton, T.L., 2021. Feature analysis, tracking, and data reduction: An application to multiphase reactor simulation mfix-exa for in-situ use case. Computing in Science and Engineering 23, 75–82. doi:10.1109/MCSE.2020.3016927.
- Biswas, A., Dutta, S., Shen, H.W., Woodring, J., 2013. An information-aware framework for exploring multivariate data sets. IEEE Transactions on Visualization and Computer Graphics 19, 2683–2692. doi:10.1109/TVCG.2013.133.
- Bramon, R., Boada, I., Bardera, A., Rodríguez, J., Feixas, M., Puig, J., Sbert, M., 2012. Multimodal data fusion based on mutual information. IEEE Transactions on Visualization and Computer Graphics 18, 1574–1587. doi:10.1109/TVCG.2011.280.
- Bramon, R., Ruiz, M., Bardera, A., Boada, I., Feixas, M., Sbert, M., 2013a. An information-theoretic observation channel for volume visualization. Computer Graphics Forum 32, 411–420. doi:10.1111/cgf.12128.
- Bramon, R., Ruiz, M., Bardera, A., Boada, I., Feixas, M., Sbert, M., 2013b. Information theory-based automatic multimodal transfer function design. IEEE Journal of Biomedical and Health Informatics 17, 870–880. doi:10.1109/JBHI.2013.2263227.
- Brewitz, A., Eickhoff, S., Dähling, S., Quast, T., Bedoui, S., Kroczeck, R.A., Kurts, C., Garbi, N., Barchet, W., Iannacone, M., et al., 2017. Cd8+ t cells orchestrate pdc-xcr1+ dendritic cell spatial and functional cooperativity to optimize priming. Immunity 46, 205–219.
- Bruckner, S., Möller, T., 2010. Isosurface similarity maps, in: Computer Graphics Forum, Wiley Online Library. pp. 773–782.
- Butts, D.A., 2003. How much information is associated with a particular stimulus? Network: Computation in Neural Systems 14, 177–187. doi:10.1088/0954-898X/14_2_301.
- Cahill, N.D., 2010. Normalized measures of mutual information with general definitions of entropy for multimodal image registration. Lecture Notes in Computer Science (including subseries Lecture Notes in Artificial Intelligence and Lecture Notes in Bioinformatics) 6204 LNCS, 258–268. doi:10.1007/978-3-642-14366-3_23.
- Camplani, M., Maddalena, L., Moyá Alcover, G., Petrosino, A., Salgado, L., 2017. A Benchmarking Framework for Background Subtraction in RGBD Videos. Lecture Notes in Computer Science (including subseries Lecture Notes in Artificial Intelligence and Lecture Notes in Bioinformatics) 10590 LNCS, 219–229. doi:10.1007/978-3-319-70742-6_21.
- Cappello, F., Di, S., Li, S., Liang, X., Gok, A.M., Tao, D., Yoon, C.H., Wu, X.C., Alexeev, Y., Chong, F.T., 2019. Use cases of lossy compression for floating-point data in scientific data sets. The International Journal of High Performance Computing Applications 33, 1201–1220.
- Castanedo, F., et al., 2013. A review of data fusion techniques. The scientific world journal 2013.
- Chen, B., Huang, B., Xu, B., 2015. Comparison of spatiotemporal fusion models: A review. Remote Sensing 7, 1798–1835.
- Chen, M., Feixas, M., Viola, I., Bardera, A., Shen, H.W., Sbert, M., 2016. Information theory tools for visualization. CRC Press.
- Childs, H., 2015. Data exploration at the exascale. Supercomputing frontiers and innovations 2, 5–13.
- Church, K., Hanks, P., 1990. Word association norms, mutual information, and lexicography. Computational linguistics 16, 22–29.
- Cover, T.M., Thomas, J.A., 2006. Elements of Information Theory 2nd Edition (Wiley Series in Telecommunications and Signal Processing). Wiley-Interscience.
- DeWeese, M.R., Meister, M., 1999. How to measure the information gained from one symbol. Network: Computation in Neural Systems doi:10.1088/0954-898X/10_4_303.
- Di, S., Cappello, F., 2016. Fast error-bounded lossy hpc data compression with sz, in: 2016 IEEE International Parallel and Distributed Processing Symposium (IPDPS), IEEE. pp. 730–739.
- Dunn, K.W., Kamocka, M.M., McDonald, J.H., 2011. A practical guide to evaluating colocalization in biological microscopy. American Journal of Physiology-Cell Physiology 300, C723–C742.
- Dutta, S., Biswas, A., Ahrens, J., 2019. Multivariate Pointwise Information-Driven Data Sampling and Visualization. Entropy 21, 699. doi:10.3390/e21070699.
- Dutta, S., Chen, C.M., Heinlein, G., Shen, H.W., Chen, J.P., 2016. In situ distribution guided analysis and visualization of transonic jet engine simulations. IEEE transactions on visualization and computer graphics 23, 811–820.
- Dutta, S., Liu, X., Biswas, A., Shen, H.W., Chen, J.P., 2017a. Pointwise information guided visual analysis of time-varying multi-fields. SIGGRAPH Asia 2017 Symposium on Visualization, SA 2017 doi:10.1145/

- 3139295.3139298.
- Dutta, S., Shen, H.W., 2016. Distribution Driven Extraction and Tracking of Features for Time-varying Data Analysis. *IEEE Transactions on Visualization and Computer Graphics* 22, 837–846. doi:10.1109/TVCG.2015.2467436.
- Dutta, S., Tasnim, H., Turton, T.L., Ahrens, J., 2021. In Situ Adaptive Spatio-Temporal Data Summarization. *Proceedings - 2021 IEEE International Conference on Big Data, Big Data 2021*, 315–321 doi:10.1109/BigData52589.2021.9671581.
- Dutta, S., Turton, T., Rogers, D., Musser, J.M., Ahrens, J., Almgren, A.S., 2022. In situ feature analysis for large-scale multiphase flow simulations. *Journal of Computational Science* 63, 101773. URL: <https://doi.org/10.1016/j.jocs.2022.101773>, doi:10.1016/j.jocs.2022.101773.
- Dutta, S., Woodring, J., Shen, H.W., Chen, J.P., Ahrens, J., 2017b. Homogeneity guided probabilistic data summaries for analysis and visualization of large-scale data sets. *IEEE Pacific Visualization Symposium*, 111–120 doi:10.1109/PACIFICVIS.2017.8031585.
- Duzceker, A., Galliani, S., Vogel, C., Speciale, P., Dusmanu, M., Pollefeys, M., 2021. Deepvideomvs: Multi-view stereo on video with recurrent spatio-temporal fusion, in: *Proceedings of the IEEE/CVF Conference on Computer Vision and Pattern Recognition*, pp. 15324–15333.
- Fu, Y., Guo, Y., Zhu, Y., Liu, F., Song, C., Zhou, Z.H., 2010. Multi-view video summarization. *IEEE Transactions on Multimedia* 12, 717–729.
- Gonzales, R.C., Wintz, P., 1987. *Digital image processing*. Addison-Wesley Longman Publishing Co., Inc.
- Gray, R.M., 2011. *Entropy and information theory*. Springer Science & Business Media.
- Haidacher, M., Bruckner, S., Kanitsar, A., Gröller, M.E., 2008. Information-based transfer functions for multimodal visualization. *EG VCBM 2008 - Eurographics Workshop on Visual Computing for Biomedicine*, 101–108.
- Hill, D.L., Batchelor, P.G., Holden, M., Hawkes, D.J., 2001. Medical image registration. *Physics in medicine & biology* 46, R1.
- Hu, W., Xie, N., Li, L., Zeng, X., Maybank, S., 2011. A survey on visual content-based video indexing and retrieval. *IEEE Transactions on Systems, Man, and Cybernetics, Part C (Applications and Reviews)* 41, 797–819.
- Isola, P., Zoran, D., Krishnan, D., Adelson, E.H., 2014. Crisp boundary detection using pointwise mutual information. *Lecture Notes in Computer Science (including subseries Lecture Notes in Artificial Intelligence and Lecture Notes in Bioinformatics)* 8691 LNCS, 799–814. doi:10.1007/978-3-319-10578-9_52.
- Kashinath, S.A., Mostafa, S.A., Mustapha, A., Mahdin, H., Lim, D., Mahmoud, M.A., Mohammed, M.A., Al-Rimy, B.A.S., Fudzee, M.F.M., Yang, T.J., 2021. Review of data fusion methods for real-time and multi-sensor traffic flow analysis. *IEEE Access* 9, 51258–51276.
- Kullback, S., Leibler, R.A., 1951. On information and sufficiency. *The annals of mathematical statistics* 22, 79–86.
- Kuruvilla, J., Sukumaran, D., Sankar, A., Joy, S.P., 2016. A review on image processing and image segmentation, in: *2016 International Conference on Data Mining and Advanced Computing (SAPIENCE)*, pp. 198–203. doi:10.1109/SAPIENCE.2016.7684170.
- Li, J., Li, Y., He, L., Chen, J., Plaza, A., 2020. Spatio-temporal fusion for remote sensing data: An overview and new benchmark. *Science China Information Sciences* 63, 1–17.
- Ma, P., Kang, E.L., 2020. Spatio-temporal data fusion for massive sea surface temperature data from modis and amsr-e instruments. *Environmetrics* 31, e2594.
- Maes, F., Collignon, A., Vandermeulen, D., Marchal, G., Suetens, P., 1997. Multimodality image registration by maximization of mutual information. *IEEE transactions on Medical Imaging* 16, 187–198.
- Mempel, T.R., Henrickson, S.E., Von Andrian, U.H., 2004. T-cell priming by dendritic cells in lymph nodes occurs in three distinct phases. *Nature* 427, 154–159.
- Mirsky, H.P., Miller, M.J., Linderman, J.J., Kirschner, D.E., 2011. Systems biology approaches for understanding cellular mechanisms of immunity in lymph nodes during infection. *Journal of theoretical biology* 287, 160–170.
- Moore, D.G., Valentini, G., Walker, S.I., Levin, M., 2018. Inform: Efficient information-theoretic analysis of collective behaviors. *Frontiers Robotics AI* 5, 1–14. doi:10.3389/frobt.2018.00060.
- Mrass, P., Oruganti, S.R., Fricke, G.M., Tafoya, J., Byrum, J.R., Yang, L., Hamilton, S.L., Miller, M.J., Moses, M.E., Cannon, J.L., 2017. Rock regulates the intermittent mode of interstitial t cell migration in inflamed lungs. *Nature communications* 8, 1010.
- Musser, J., Almgren, A.S., Fullmer, W.D., Antepará, O., Bell, J.B., Blaschke, J., Gott, K., Myers, A., Porcu, R., Rangarajan, D., Rosso, M., Zhang, W., Syamlal, M., 2022. MFix-Exa: A path toward exascale CFD-DEM simulations. *International Journal of High Performance Computing Applications* 36, 40–58. doi:10.1177/10943420211009293.
- Myers, K., Lawrence, E., Fugate, M., Bowen, C.M., Ticknor, L., Woodring, J., Wendelberger, J., Ahrens, J., 2016. Partitioning a large simulation as it runs. *Technometrics* 58, 329–340.
- Nguyen, H., Katzfuss, M., Cressie, N., Braverman, A., 2014. Spatio-temporal data fusion for very large remote sensing datasets. *Technometrics* 56, 174–185.
- Pilkiewicz, K.R., Lemasson, B.H., Rowland, M.A., Hein, A., Sun, J., Berdahl, A., Mayo, M.L., Moehlis, J., Porfiri, M., Fernández-Juricic, E., Garnier, S., Bollt, E.M., Carlson, J.M., Tarampi, M.R., MacÚga, K.L., Rossi, L., Shen, C.C., 2020. Decoding collective communications using information theory tools. *Journal of the Royal Society Interface* 17. doi:10.1098/rsif.2019.0563.
- Reed, D.A., Dongarra, J., 2015. Exascale computing and big data. *Communications of the ACM* 58, 56–68.
- RGBD2017, . Background learning for detection and tracking from rgbd videos. <https://rgbd2017.na.icar.cnr.it/>. Accessed: 2023-09-22.
- Rubart, M., 2004. Two-photon microscopy of cells and tissue. *Circulation research* 95, 1154–1166.
- Ruiz, M., Bardera, A., Boada, I., Viola, I., Feixas, M., Sbert, M., 2011. Automatic transfer functions based on informational divergence. *IEEE Transactions on Visualization and Computer Graphics* 17, 1932–1941. doi:10.1109/TVCG.2011.173.
- Sbert, M., Feixas, M., Rigau, J., Chover, M., Viola, I., 2022. Information theory tools for computer graphics. *Springer Nature*.
- SBM-RGBD Dataset, . Sbm-rgbd dataset. <https://rgbd2017.na.icar.cnr.it/SBM-RGBDdataset.html>. Accessed: 2023-09-22.
- Schroeder, W., Martin, K.M., Lorensen, W.E., 1998. *The visualization toolkit an object-oriented approach to 3D graphics*. Prentice-Hall, Inc.
- Shah, Z., Anwar, A., Mahmood, A.N., Tari, Z., Zomaya, A.Y., 2017. A spatiotemporal data summarization approach for real-time operation of smart grid. *IEEE Transactions on Big Data* 6, 624–637.
- Shannon, C.E., 1948. A Mathematical Theory of Communication. *Bell System Technical Journal* 27, 379–423. doi:10.1002/j.1538-7305.1948.tb01338.x.
- Sipser, M., 2013. *Introduction to the Theory of Computation*. Third ed., Course Technology, Boston, MA.
- Tang, Y., Wang, Q., Zhang, K., Atkinson, P.M., 2020. Quantifying the effect of registration error on spatio-temporal fusion. *IEEE Journal of Selected Topics in Applied Earth Observations and Remote Sensing* 13, 487–503.
- Tasnim, H., Dutta, S., Turton, T.L., Rogers, D.H., Moses, M.E., 2022. Information-Theoretic Exploration of Multivariate Time-Varying Image Databases. *Computing in Science and Engineering* 24, 61–70. doi:10.1109/MCSE.2022.3188291.
- Tasnim, H., Fricke, G., Byrum, J., Sotiris, J., Cannon, J., Moses, M., 2018. Quantitative measurement of naïve T cell association with dendritic cells, FRCs, and blood vessels in lymph nodes. *Frontiers in Immunology* 9. doi:10.3389/fimmu.2018.01571.
- Tong, X., Lee, T.Y., Shen, H.W., 2012. Salient time steps selection from large scale time-varying data sets with dynamic time warping, in: *IEEE symposium on large data analysis and visualization (LDAV)*, IEEE. pp. 49–56.
- Verdu, S., 1998. Fifty years of shannon theory. *IEEE Transactions on Information Theory* 44, 2057–2078. doi:10.1109/18.720531.
- Vidhya, K., Karthikeyan, G., Divakar, P., Ezhumalai, S., 2016. A review of lossless and lossy image compression techniques. *Int. Res. J. Eng. Technol.(IRJET)* 3, 616–7.

- Viola, I., Feixas, M., Sbert, M., Groller, M.E., 2006. Importance-driven focus of attention. *IEEE transactions on visualization and computer graphics* 12, 933–940.
- Viola, P., Wells III, W.M., 1997. Alignment by maximization of mutual information. *International journal of computer vision* 24, 137–154.
- Wang, C., Yu, H., Ma, K.L., 2008. Importance-driven time-varying data visualization. *IEEE Transactions on Visualization and Computer Graphics* 14, 1547–1554.
- Wang, Q., Tang, Y., Tong, X., Atkinson, P.M., 2020. Virtual image pair-based spatio-temporal fusion. *Remote Sensing of Environment* 249, 112009.
- Wei, T.H., Dutta, S., Shen, H.W., 2018. Information guided data sampling and recovery using bitmap indexing, in: 2018 IEEE Pacific Visualization Symposium (PacificVis), IEEE. pp. 56–65.
- Woodring, J., Ahrens, J., Figg, J., Wendelberger, J., Habib, S., Heitmann, K., 2011. In-situ sampling of a large-scale particle simulation for interactive visualization and analysis, in: *Computer Graphics Forum*, Wiley Online Library. pp. 1151–1160.
- Wu, P., Yin, Z., Zeng, C., Duan, S.B., Göttsche, F.M., Ma, X., Li, X., Yang, H., Shen, H., 2021. Spatially continuous and high-resolution land surface temperature product generation: A review of reconstruction and spatiotemporal fusion techniques. *IEEE Geoscience and Remote Sensing Magazine* 9, 112–137.
- Xue, J., Leung, Y., Fung, T., 2017. A bayesian data fusion approach to spatio-temporal fusion of remotely sensed images. *Remote Sensing* 9, 1310.
- Ye, Y.C., Neuroth, T., Sauer, F., Ma, K.L., Borghesi, G., Konduri, A., Kolla, H., Chen, J., 2016. In situ generated probability distribution functions for interactive post hoc visualization and analysis, in: 2016 IEEE 6th Symposium on Large Data Analysis and Visualization (LDAV), IEEE. pp. 65–74.
- Zhang, L., Gao, Y., Hong, R., Hu, Y., Ji, R., Dai, Q., 2014. Probabilistic skimlets fusion for summarizing multiple consumer landmark videos. *IEEE Transactions on Multimedia* 17, 40–49.
- Zhong, S.h., Wu, J., Jiang, J., 2019. Video summarization via spatio-temporal deep architecture. *Neurocomputing* 332, 224–235.
- Zhou, B., Chiang, Y.J., 2018. Key time steps selection for large-scale time-varying volume datasets using an information-theoretic storyboard, in: *Computer Graphics Forum*, Wiley Online Library. pp. 37–49.